Received: 10 July 2023 | Revised: 3 November 2023 | Accepted: 6 November 2023

DOI: 10.1002/pro.4835

RESEARCH ARTICLE

THE PROTEIN SOCIETY WILEY

Exploring protein–protein interactions and oligomerization state of pulmonary surfactant protein C (SP-C) through FRET and fluorescence self-quenching

Mishelle Morán-Lalangui[1,2] | **Ana Coutinho**[3,4,5] | **Manuel Prieto**[3,4] | **Alexander Fedorov**[3,4] | **Jesús Pérez-Gil**[1,2] | **Luís M. S. Loura**[6,7,8] | **Begoña García-Álvarez**[1,2,9]

[1]Department of Biochemistry and Molecular Biology, Faculty of Biology, Complutense University, Madrid, Spain

[2]Research Institute "Hospital 12 de Octubre (imas12)", Madrid, Spain

[3]iBB Institute for Bioengineering and Bioscience, IST, Universidade de Lisboa, Lisbon, Portugal

[4]Associate Lab i4HB, Institute for Health and Bioeconomy at IST, Universidade de Lisboa, Lisbon, Portugal

[5]Department of Chemistry and Biochemistry, Faculty of Sciences, University of Lisbon, Lisbon, Portugal

[6]Department of Chemistry, Coimbra Chemistry Centre, Institute of Molecular Sciences (CQC-IMS), University of Coimbra, Coimbra, Portugal

[7]CNC Centre for Neuroscience and Cell Biology, University of Coimbra, Coimbra, Portugal

[8]Faculty of Pharmacy, University of Coimbra, Coimbra, Portugal

[9]Department of Biochemistry and Molecular Biology, Faculty of Chemistry, Complutense University, Madrid, Spain

Correspondence
Luís M. S. Loura, Department of Chemistry, Coimbra Chemistry Centre, Institute of Molecular Sciences (CQC-IMS), University of Coimbra, Coimbra, Portugal.
Email: lloura@ff.uc.pt

Abstract

Pulmonary surfactant (PS) is a lipid–protein complex that forms films reducing surface tension at the alveolar air–liquid interface. Surfactant protein C (SP-C) plays a key role in rearranging the lipids at the PS surface layers during breathing. The N-terminal segment of SP-C, a lipopeptide of 35 amino acids, contains two palmitoylated cysteines, which affect the stability and structure of the molecule. The C-terminal region comprises a transmembrane α-helix that contains a ALLMG motif, supposedly analogous to a well-studied dimerization motif in glycophorin A. Previous studies have demonstrated the potential interaction between SP-C molecules using approaches such as Bimolecular Complementation assays or computational simulations. In this work, the oligomerization state of SP-C in membrane systems has been studied using fluorescence spectroscopy techniques. We have performed self-quenching and FRET assays to analyze dimerization of native palmitoylated SP-C and a non-palmitoylated recombinant version of SP-C (rSP-C) using fluorescently labeled versions of either protein reconstituted in different lipid systems mimicking pulmonary surfactant environments. Our results reveal that doubly palmitoylated native SP-C remains primarily monomeric. In contrast, non-palmitoylated recombinant SP-C exhibits dimerization, potentiated at high concentrations, especially in membranes with lipid phase separation. Therefore, palmitoylation could play a crucial role in stabilizing the monomeric α-helical conformation of SP-C. Depalmitoylation, high protein densities as a consequence of membrane compartmentalization, and other factors may all lead to the formation of protein dimers and higher-order oligomers, which could have functional implications under certain pathological conditions and contribute to membrane transformations associated with surfactant metabolism and alveolar homeostasis.

Begoña García-Álvarez, Department of Biochemistry and Molecular Biology, Faculty of Biology, Complutense University, Madrid, Spain.
Email: begoga01@ucm.es

Funding information
Comunidad de Madrid, Grant/Award Number: P2018/NMT-4389; European Biophysical Societies' Association (EBSA); Fundação para a Ciência e a Tecnologia, Grant/Award Numbers: UIDB/00313/2020, UIDP/00313/2020, UIDB/04565/2020, UIDP/04565/2020, LA/P/0140/2020; Ministerio de Ciencia e Innovación, Grant/Award Number: PID2021-124932OB-100

Review Editor: Aitziber L. Cortajarena

KEYWORDS
FRET, oligomerization state, protein–protein interaction, pulmonary surfactant, self-quenching, surfactant protein C (SP-C)

1 | INTRODUCTION

The alveoli are responsible for gas exchange between the air in the lungs and the bloodstream. They are coated by two main types of alveolar cells: type I (AT1) cells, which comprise about 95% of the alveolus surface and type II (AT2) cells encompassing the remaining 5%, approximately (Guillot et al., 2013). AT1 cells are thin and flat cells that take part in the exchange of gases while AT2 cells have a cuboidal morphology and secrete Pulmonary Surfactant (PS). The PS is a lipid-protein multilayered complex that forms films lining the alveolar surface and reduce surface tension (Goerke, 1998). Once synthesized in the endoplasmic reticulum, PS is assembled into lamellar bodies (LBs), which once secreted are rapid and efficiently adsorbed into the air–liquid interface. In this way, PS film is the first physical contact with harmful particles inhaled during breathing and contributes to the innate defense system of the lung (Chroneos et al., 2010). Both biophysical and immunological functions of PS depend on its composition which is mainly lipids (90% of PS mass), particularly saturated lipids as dipalmitoyl phosphatidylcholine (DPPC, 40%), unsaturated lipids (35%), and neutral lipids as cholesterol (8%–10%) (Daniels & Orgeig, 2003). The remaining 10% of PS mass encompasses surfactant proteins (SPs): SP-A, SP-B, SP-C, and SP-D (Daniels & Orgeig, 2003; Goerke, 1998). They are essential for a proper function of the lung (Griese, 1999).

SP-A and SP-D are hydrophilic proteins, members of the collection family of proteins that are involved in innate immunity (Ariki et al., 2012; Perez-Gil & Weaver, 2010). Deficiency or dysfunction of SP-A and SP-D has been associated with various lung disorders, including acute respiratory distress syndrome (ARDS) and chronic obstructive pulmonary disease (COPD) (Mason et al., 1998; Perez-Gil & Weaver, 2010; Silveyra & Floros, 2012). On the other hand, SP-B and SP-C are small cationic and highly hydrophobic proteins (Daniels & Orgeig, 2003; Goerke, 1998). They are essential for the biophysical function of PS due to their ability to rearrange lipids from PS membranes and interfacial films during compression–expansion breathing cycles (Parra & Pérez-Gil, 2015; Serrano & Pérez-Gil, 2006). Lack of SP-B results in respiratory failure and death shortly after birth, while SP-C deficiency causes lung failure at long term (Amin et al., 2001; Clark et al., 1995; Nogee et al., 1994; Tokieda et al., 1997).

The main activity of SP-C consists of the transference of lipids between the lipid monolayer at the air–liquid interface and multilayered membrane reservoirs beneath the monolayer. Additionally, SP-C is able to interact with lipopolysaccharide (LPS) of Gram-negative bacteria as well as CD14 of macrophages, a co-receptor of bacterial LPS (Augusto et al., 2001; Augusto et al., 2002; Augusto, Synguelakis, Johansson, et al., 2003). Different evidences indicate that SP-C may play an anti-inflammatory role, as demonstrated by its ability to decrease levels of inflammatory mediators, including tumoral necrosis factor α (TNF-α) and nitric oxide, induced by LPS (Augusto, Synguelakis, Espinassous, et al., 2003; Garcia-Verdugo et al., 2009). Thus, SP-C could play a relevant role modulating the immune response against pathogens and maintaining alveolar homeostasis. SP-C is synthetized as a large precursor of 197 amino acid residues (21 kDa) that includes a BRICHOS domain that contributes to a proper folding and palmitoylation of the protein (ten Brinke, Vaandrager, et al., 2002; ten Brinke, van Golde, & Batenburg, 2002). This precursor is processed along the SP-B precursor within the lamellar bodies of AT2 cells (Olmeda et al., 2017; ten Brinke, van Golde, & Batenburg, 2002; Weaver, 1998). Mature SP-C is the

smallest protein of PS (4.2 kDa), composed just by 35 amino acids (FGIPCCPVHLKRLLIVVVVVVLIVV VIVGALLMGL in *Homo sapiens*), and encompasses about 1% of PS mass (Daniels & Orgeig, 2003; Goerke, 1998; Johansson, 1998). It adopts a transmembrane α-helical structure despite its high proportion of aliphatic branched residues, such as valines, typically promoting formation of β sheets (Chou & Fasman, 1978). These residues confer an extreme stiffness to the α-helix (Johansson et al., 1994). The N-terminal segment of SP-C, constituted by the first 12 amino acids, is not in principle embedded into the membrane and adopts an undefined structure (Johansson, 1998; Plasencia et al., 2001; Vandenbussche et al., 1992). However, it is able to interact with anionic lipids of PS layers, such as phosphatidylglycerol (PG), due to its cationic charge. Moreover, cysteine residues of this segment are stoichiometrically palmitoylated (Johansson, 1998; ten Brinke, van Golde, & Batenburg, 2002). Palmitoylation has been shown to affect the stability and structure of the protein. It also allows the anchoring of the N-terminal segment to the membrane, modulating SP-C tilting in lipid bilayers. Furthermore, palmitoylated SP-C is more resistant to proteolytic degradation (Dluhy et al., 2003; Roldan et al., 2015; Vandenbussche et al., 1992; Wang et al., 1996). The C-terminal region of SP-C comprises the transmembrane α-helix that contains a ALLMG motif. It has been proposed as a dimerization domain analogous to the GxxxG motif present in the membrane protein glycophorin A (GpA), whose homodimerization state has been extensively characterized (Kairys et al., 2004; Luy et al., 2004; Sarabipour & Hristova, 1828). Both sequences are conserved among a wide range of species including human SP-C and porcine SP-C. Recently, Barriga et al. have shown that SP-C molecules could interact with each other using bimolecular fluorescence complementation assays (BiFC) (Barriga et al., 2021). However, this technique does not allow discerning between a purely dimeric or an oligomeric structure (Hiatt et al., 2008; Jia et al., 2021). In addition, Korolainen et al. have studied through molecular dynamics simulations the potential dimerization of SP-C and they have proposed that SP-C dimerization could depend on a sequence motif larger than AxxxG (Korolainen et al., 2022).

In this work, the oligomerization state of SP-C in membrane systems was studied using fluorescence spectroscopy techniques. Our results show that native doubly palmitoylated SP-C was not able to form dimers or oligomers in POPC membranes where compartmentalization is not possible, in contrast to non-palmitoylated recombinant SP-C, which could dimerize at high concentrations, particularly in the presence of a lipid phase separation.

2 | RESULTS

The absorption and emission spectra of SP-C labeled with Marina Blue or BODIPY-FL fluorophores upon incorporation into POPC bilayers under diluted conditions are depicted in Figure 1. No significant spectral alterations were detected for BODIPY SP-C compared to BODIPY SP-B (Umberger & LaMer, 1945), and these spectral profiles are also identical to the ones obtained with the recombinant SP-C protein, rSP-C (results not shown). Upon direct inspection of Figure 1, a large overlap between Marina Blue fluorescence emission and BODIPY-FL absorption spectra can be detected, allowing for an efficient FRET interaction. Incorporating fluorophores into a biological structure could influence on the intrinsic structure. To study this issue, we have performed circular dichroism (CD) measurements.

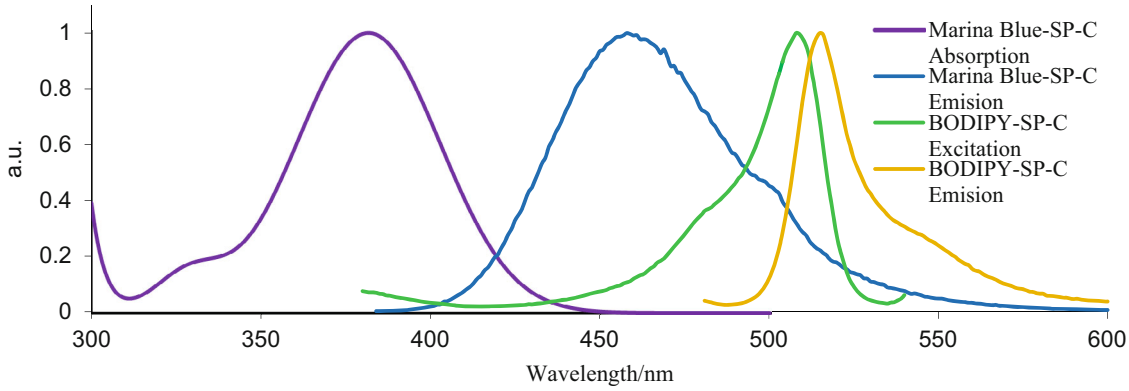

FIGURE 1 Normalized spectra of Marina Blue SP-C and BODIPY SP-C in POPC membranes. The spectra were obtained with 0.5 mol% of Marina Blue SP-C (Cabre et al., 2018), and 0.125 mol% of BODIPY SP-C in 1 mM POPC vesicles.

TABLE 1 Fluorescence intensity and anisotropy decay fitting parameters for fluorescently-labeled Marina Blue SP-C and BODIPY SP-C in POPC membranes.

	Marina Blue SP-C	BODIPY SP-C
Fluorescence intensity decay parameters		
τ_1/ns	0.23 (0.26)	6.0 (1.0)
τ_2/ns	1.9 (0.17)	—
τ_3/ns	5.3 (0.57)	—
χ^2	1.088	1.115
Fluorescence anisotropy decay parameters		
ϕ_1/ns	0.79 (0.3)	1.2 (0.43)
ϕ_2/ns	21.0 (0.69)	14.1 (0.57)
χ^2	1.205	1.219

Note: The parameters (with normalized amplitudes inside parentheses) have been determined in samples containing 0.5 mol% Marine Blue SP-C or 0.125 mol% BODIPY SP-C in 1 mM POPC vesicles. τ_i are the lifetimes components and ϕ_i the rotational correlation times. See text for further details.

Deconvolution of spectra profiles has shown that the probe does not disrupt the essentially alpha-helical structure of the protein (results not shown).

The photophysical characterization of these two derivatized proteins is presented in Table 1 and Figure 2. The fluorescence intensity decay of Marina Blue SP-C is well described by three exponentials, with an additional faster component when compared with previous data (Cabre et al., 2018). A similar behavior was obtained for the fluorescence anisotropy decay of Marina Blue SP-C, where the previous limiting anisotropy is now translated by a very long rotational correlation time $\phi = 21.0$ ns. For the BODIPY SP-C, its fluorescence intensity decay is successfully described by a single exponential of $\tau = 6.0$ ns, and a long rotational correlation time of $\phi = 14.1$ ns is necessary to adequately fit its fluorescence anisotropy decay. It should be stressed that these results are essentially identical to the ones previously described in (Cabre et al., 2018), and the small differences are essentially due to a better instrumental time-resolution, allowing for the

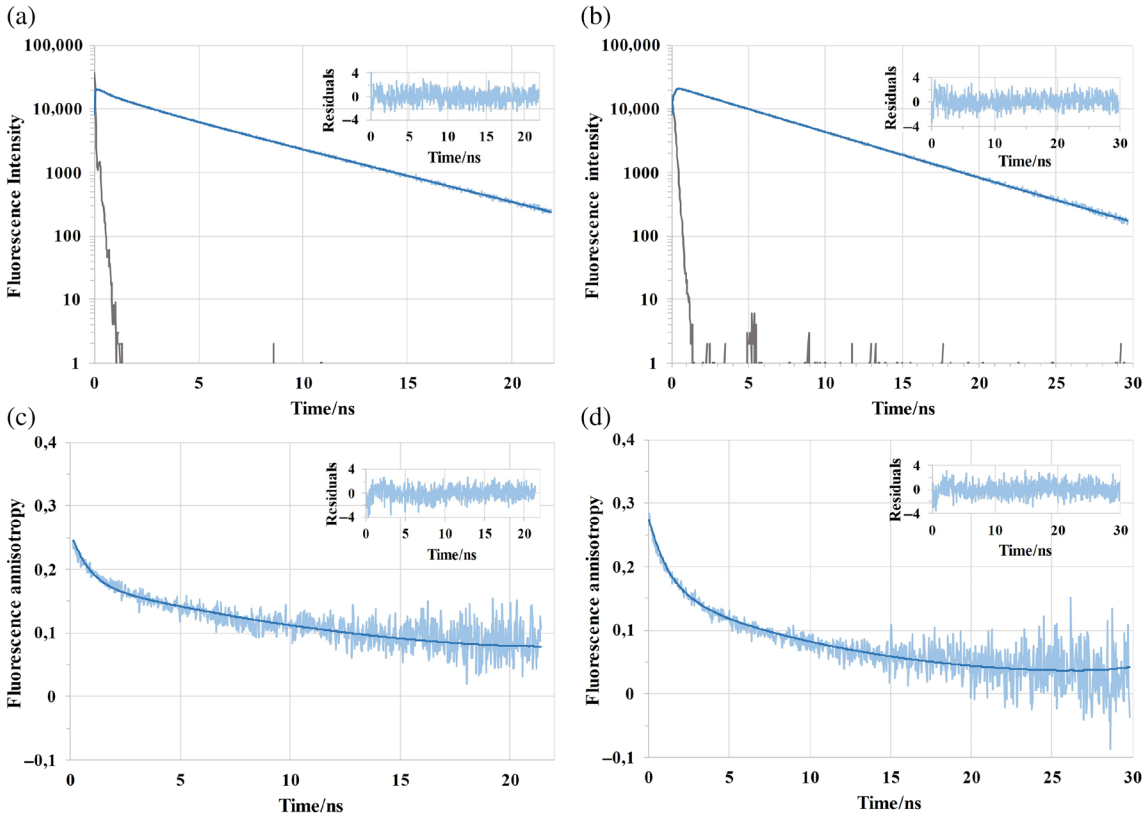

FIGURE 2 Fluorescence intensity and anisotropy decays of Marina Blue SP-C and BODIPY SP-C in POPC membranes. (a,b) Fluorescence intensity and (c,d) anisotropy decays of (a,c) Marina Blue SP-C, and (b,d) BODIPY SP-C in POPC vesicles (see Table 1 for probe:lipid ratios). Solid dark lines represent the best fitting curves using the fitting parameters of Table 1. The distributions of residues are shown in the *inset plots*.

detection of ultrafast components in the fluorescence intensity decays.

2.1 | Protein lateral diffusion and compartmentalization from time-resolved self-quenching

The self-quenching (SQ) of emission of the BODIPY fluorophore upon aggregation and π-stacking interactions has been reported often in the literature (e.g., Kang et al., 2022; Liu et al., 2019; Pakhomov et al., 2017). In the present work, we used both time-resolved and steady-state self-quenching (TRSQ and SSSQ, respectively) as means to probe the lateral diffusion/compartmentalization (from TRSQ) and aggregation (from SSSQ) of the two fluorescently labeled proteins in the different lipid systems. We address the former in this subsection.

The dependence of BODIPY SP-C and BODIPY rSP-C mean fluorescence lifetimes on their membrane concentrations were analyzed using a Stern–Volmer equation:

$$\overline{\tau}_0/\overline{\tau} = 1 + k_q\langle\tau_0\rangle[Q], \tag{1}$$

where $[Q]$ is the fluorophore concentration in the lipid phase (equal to that of the fluorescently labeled protein, corrected for the corresponding labeling ratio), $\overline{\tau}$ is the amplitude-averaged mean fluorescence lifetime,

$$\overline{\tau} = \sum_i \alpha_i \tau_i, \tag{2}$$

and $<\tau>$ is the intensity-averaged mean fluorescence lifetime,

$$\langle\tau\rangle = \frac{\sum_i \alpha_i \tau_i^2}{\sum_i \alpha_i \tau_i}, \tag{3}$$

The subscript "0" indicates values extrapolated to infinite dilution. The main fitting parameter in the Stern–Volmer plots is the bimolecular collisional quenching rate constant, k_q. According to the approximation of Umberger and Lamer (1945), it is related to the self-diffusion coefficient D through

$$k_q = 4\pi N_A (2R_c)(2D)\left(1 + \frac{2R_c}{\sqrt{2\langle\tau_0\rangle D}}\right), \tag{4}$$

where N_A is the Avogadro constant and R_c is the collisional radius, which for self-quenching equals to twice the fluorophore radius.

Stern–Volmer plots for the different systems under study are depicted in Figure 3. Note the enlarged ordinate scale in the right plots, indicative of a larger extent of self-quenching for rSP-C, especially in the LM (mixture of DPPC/POPC/POPG, 50/25/15 w/w/w) and LS (full lipid surfactant) systems. Table 2 shows the corresponding D values obtained from solving the non-linear Equation (4) (with $R_c = 1.0$ nm), as well as their 90% confidence intervals. The diffusion coefficient measured for BODIPY SP-C in POPC is typical of a membrane-inserted protein, being in fact similar to that previously obtained for BODIPY SP-B in the same system (Cabre et al., 2018), and of the order of what is expected for phospholipids in fluid disordered bilayers ($\sim 10^{-7}$ cm^2/s; Filippov et al., 2003, 2004). A similar extent of dynamic self-quenching, and consequently a similar D value, was measured for BODIPY SP-C in the LM system. At variance, for LS membranes, a larger degree of quenching occurred within the same concentration range, implying a higher diffusion coefficient by approximately an order of magnitude. Such value is unrealistically high for lateral diffusion in lipid bilayers, and reflects compartmentalization of SP-C, resulting in much higher effective SP-C concentrations available for dynamic self-quenching than expected from the bulk membrane concentration in this system.

Turning now to BODIPY rSP-C, an approximately two-fold increase in D was observed in POPC compared to the value obtained for the palmitoylated protein. This slightly faster lateral diffusion of BODIPY rSP-C compared to BODIPY SP-C could be rationalized on account of the lack of the membrane-inserted acyl chain. On the other hand, compared to POPC, the apparent diffusion coefficient of BODIPY rSP-C is increased by a factor of ≅4 and ≅15 in LM and LS vesicles, respectively. While the results obtained for both proteins in LS are qualitatively similar, the higher apparent diffusion coefficient in LM compared to POPC reveals that BODIPY rSPC probably has a confined distribution in this lipid system, contrary to its palmitoylated counterpart.

2.2 | Protein aggregation from steady-state self-quenching

SSSQ of BODIPY-labeled membrane proteins was monitored at $\lambda_{em} = 550$ nm, following excitation at $\lambda_{em} = 470$ nm (Figure 4). The measured fluorescence intensities I_F were analyzed first with a formalism that combined dynamical with static quenching, the latter being described by an active sphere term, which accounts for transient statistical nonfluorescent contact pairs, formed at the moment of excitation, but not involved in

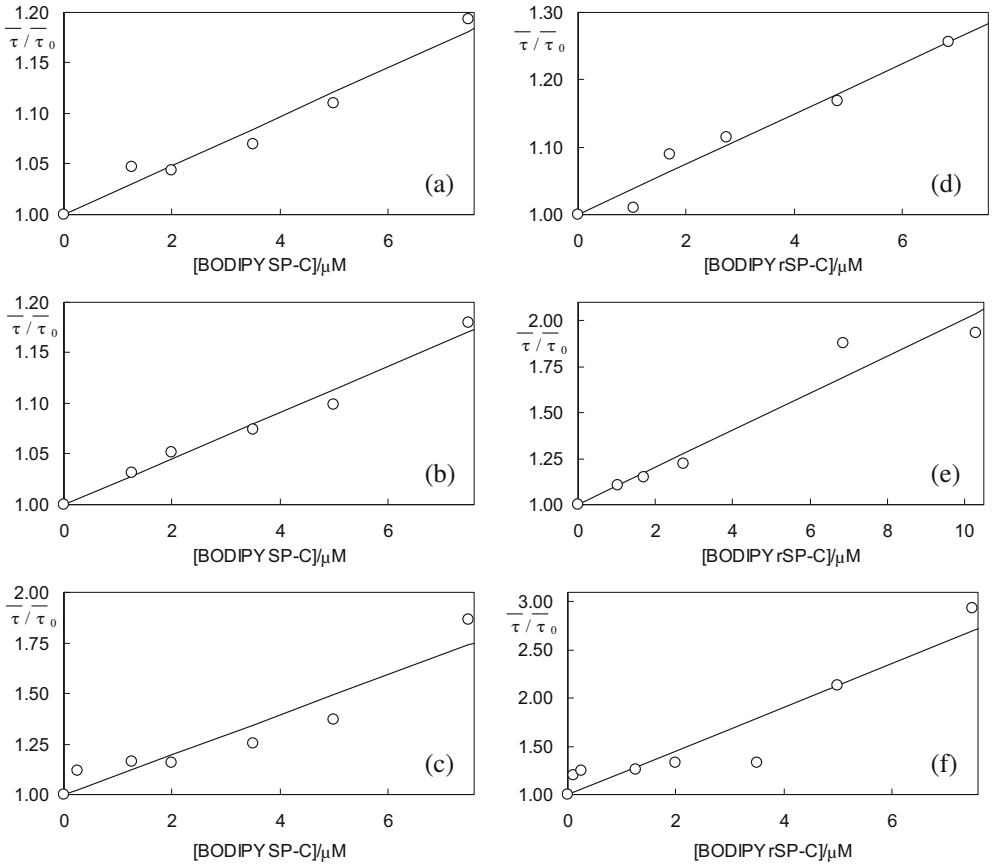

FIGURE 3 Dynamic self-quenching of BODIPY SP-C and rSP-C in membranes. Stern–Volmer plots for the dynamic self-quenching studies of BODIPY SP-C (a–c) or BODIPY rSP-C (d–f) in POPC (a,d), DPPC/POPC/POPG lipid mixture (b,e), or LS (lipid surfactant) (c,f). The solid lines are the best fits of Equation (1) to the experimental data of $\overline{\tau}/\overline{\tau}_0$ ratios (circles) as a function of the concentration of the fluorescently labeled protein used in each case. Note the enlarged ordinate scale in the right plots, indicative of a larger extent of self-quenching for BODIPY rSP-C.

TABLE 2 Lateral diffusion coefficients of BODIPY SP-C and BODIPY rSP-C in membranes.

	D (10^{-7} cm^2/s)	
System	**BODIPY SP-C**	**BODIPY rSP-C**
POPC	1.92 (1.39–2.52)	4.03 (2.97–5.19)
LM	1.55 (1.23–1.90)	15.7 (11.0–20.8)
LS	16.3 (10.8–22.1)	51.2 (42.1–60.5)

Note: The coefficient D (10^{-7} cm^2/s) has been obtained from Equation (4) after fitting Equation (1) to the Stern–Volmer plots of Figure 3 for either protein in POPC, LM (DPPC/POPC/POPG lipid mixture) or LS (lipid surfactant); 90% confidence intervals are given inside parentheses.

complexes formation (i.e., with interaction energy below the thermal value) (Cabre et al., 2018; Fernandes et al., 2003):

$$I_F = \frac{C[F]}{1/\overline{\tau}_0 + k_q[F]} \exp(-VN_A[F]). \quad (5)$$

In this equation, V is the active sphere volume and C is a multiplying factor. From this analysis, we concluded that no aggregation of BODIPY SP-C was apparent in POPC or LM bilayers (a $V = 0$ being recovered), while a low degree of aggregation was observed for this protein in LS, compatible with formation of statistical contact pairs (active sphere radius $R = (3V/(4\pi))^{1/3} = 8.9$ Å). Conversely, for BODIPY rSP-C, higher active sphere radii were retrieved in all systems, namely 13.8, 26.7, and 18.7 Å for POPC, LM, and LS, respectively. Such values, namely the latter two, are higher than the expected interfluorophore distances for a contact dimer, indicating a higher extent of aggregation than what could be justifiably rationalized as statistical pairs. This led us to alternatively consider a dimerization scheme,

$$2F_1 \rightleftharpoons F_2, K = [F_2]/[F_1]^2, [F] = [F_1] + 2[F_2], \quad (6)$$

where F_1 and F_2 represent monomeric and dimeric fluorophore species, and $[F]$ is the total fluorophore concentration. In these circumstances, the fluorescence intensity will be given by

$$I_F = \frac{C[F_1]}{1/\overline{\tau}_0 + k_q[F]}. \quad (7)$$

Solving Equation (6) for (for given K and $[F]$ values), and inserting in Equation (7) leads to (Fernandes et al., 2003):

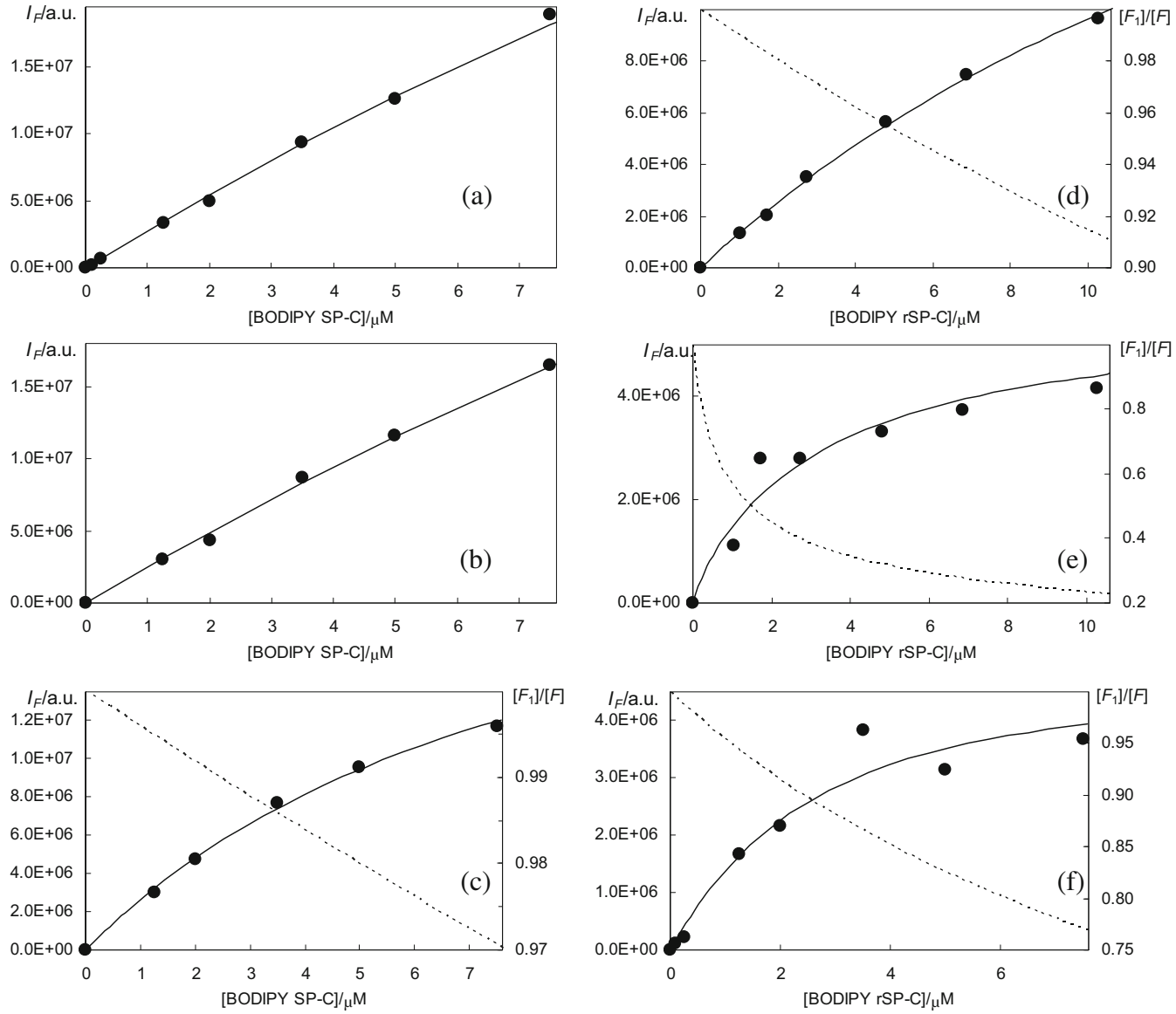

FIGURE 4 Steady-state fluorescence of BODIPY SP-C and BODIPY rSP-C in membranes. Steady-state fluorescence intensity (I_F; circles) of BODIPY SP-C (a–c) or BODIPY rSP-C (d–f) in POPC (a,d), DPPC/POPC/POPG lipid mixture (b,e), or pulmonary surfactant lipid fraction (c–f). The solid lines are the best fits to a combined dynamic and static quenching mechanism, with an active sphere (a,b; $V = 0$ in Equation (5)) or dimerization equilibrium (c–f; Equation (7), see text for K values in each case) formalism. In the latter situation, the fractions of monomeric labeled protein, $/[F]$, are plotted as dotted lines, referring to the secondary ordinate axes of the corresponding panels.

$$I_F = \frac{C}{1/\tau_0 + k_q[F]} \frac{-1+\sqrt{1+8K[F]}}{4K}. \quad (8)$$

This equation holds for the hypothetical situation of a complete protein labeling with fluorophore. However, in the case of incomplete protein labeling, such as in the present situation, three different combinations are possible for dimers, namely labeled/labeled, labeled/unlabeled, and unlabeled/unlabeled protein pairs. Only formation of the first one leads to self-quenching of BODIPY. Under this situation, the concentration of protein in each form can be obtained for a given K value by numerically solving a set of nonlinear equations, as detailed in the Appendix S1. Summing the concentration of the two species with a single labeled protein (either true monomers or unlabeled/labeled dimers) and inserting that sum in the numerator of Equation (7) (in the place of), the theoretical fluorescence intensity is obtained as a function of total protein, and from fitting of this variation to the experimental I_F, one recovers K (as well as C), which, in turn, allows estimation of the variable concentrations of the monomeric and dimeric species.

For the situations where the sphere of action formalism indicated the possibility of aggregation, namely BODIPY SP-C in LS or BODIPY rSP-C in POPC, LM, or LS membranes, we used the dimer equilibrium formalism, to obtain $K = 1.0\ M^{-1}$, $3.9\ M^{-1}$, $438\ M^{-1}$, and $16.6\ M^{-1}$, respectively. For these systems, the corresponding panels of Figure 4C–F, respectively, show the fraction of monomeric labeled protein as a function of total fluorescently labeled protein.

A critical comment should be made here about the quenching models and the best-fit values recovered: (i) there is some scatter in the data for plots E and F; (ii) there is anti-correlation between the two sources of quenching, meaning that an underestimation of the dynamic component may be counterbalanced by an overestimation of the static one, and vice versa; (iii) although the fits in Figure 4 are satisfactory, higher order aggregates cannot be ruled out; and finally (iv) for simplicity, it is assumed that the quenching efficiency of dimers involving fluorescent units is strictly unity. Still, it can be concluded that these results point to an essentially monomeric distribution of BODIPY SP-C in all systems (a very slight degree of aggregation is apparent only in LS), in contrast to BODIPY rSP-C, for which aggregation can be inferred, most significantly in the LM and LS systems.

2.3 | Protein lateral membrane distribution from time-resolved FRET measurements

The time-resolved emission of Marina Blue SP-C and Marina Blue rSP-C was measured in the absence and in the presence of varying membrane concentrations of BODIPY SP-C and BODIPY rSP-C, respectively. As clearly seen in Figure 1, the emission spectrum of Marina Blue and the absorption spectrum of BODIPY display considerable overlap. This allows for an efficient FRET between protein molecules labeled with the two fluorophores, with a Förster distance of 4.93 nm as previously determined (Cabre et al., 2018).

For each lipid system, the fluorescence intensity decays of samples with donor only (vesicles loaded with 5 μM Marina Blue SP-C or Marina Blue rSP-C) and donor + acceptor (vesicles loaded with 5 μM Marina Blue SP-C or Marina Blue rSP-C, and varying concentrations of BODIPY SP-C or BODIPY rSP-C) were measured. For each acceptor concentration, the donor-only sample received a concentration of the corresponding unlabeled protein equal to that of the BODIPY-labeled protein in the corresponding donor + acceptor sample. These two decays were analyzed globally, with linkage of the common decay parameters, as described previously in our study of SP-C/SP-B interactions (Cabre et al., 2018). In that work, we also established as the best FRET model a formalism that allows for the possibility of two populations (relative amounts A_1 and A_2) of non-equivalent donors, transferring excitation energy to corresponding populations of acceptors (with local two-dimensional concentrations c_1 and c_2, respectively). Each donor molecule can undergo FRET to acceptors located in the same bilayer leaflet (cis FRET) or in the opposite one (trans FRET), at a transverse distance $h = 3.4$ nm (see fig. 7 of Cabre et al., 2018). The donor decay in the presence of acceptor, $i_{DA}(t)$, is described by

$$i_{DA}(t) = i_D(t)\left[A_1\rho_{cis,1}(t)\rho_{trans,1}(t) + A_2\rho_{cis,2}(t)\rho_{trans,2}(t)\right], \tag{9}$$

where $i_D(t)$ is the donor decay in the absence of acceptor (described as a sum of up to three exponentials), and the ρ functions, given by

$$\rho_{cis,i}(t) = \exp\left(-c_i t^{1/3}\right), \tag{10}$$

and

$$\rho_{trans,i}(t) = \exp\left\{-\frac{2\,c_i}{\Gamma(2/3)\cdot b}\int_0^1 \left[1-\exp\left(-t\,b^3\alpha^6\right)\right]\alpha^{-3}d\alpha\right\}, \tag{11}$$

are the *cis* and *trans* FRET terms that apply to donor and acceptor population i ($i = 1, 2$).

In the latter equation, Γ is the complete gamma function and $b = (R_0/h)/<\tau_D>^{1/3}$ (Davenport et al., 1985).

From the recovered acceptor concentrations c_1 and c_2, an overall acceptor concentration $<c>$ may be calculated obtained by averaging with weights given by the relative amount of donors ($q = A_2/A_1$):

$$\langle c\rangle = (c_1 + qc_2)/(1+q), \tag{12}$$

which can be compared with the theoretical expectation, obtained from the two-dimensional acceptor concentration n (molecules/unit area) (Loura et al., 1996, 2000):

$$c = n\Gamma(2/3)\pi R_0^2/\langle\tau_D\rangle^{1/3}. \tag{13}$$

As an example, Figure 5 shows experimental decays, fitting curves, as well as residual distributions and residual autocorrelations, for the Marina Blue SP-C/BODIPY SP-C FRET pair in POPC. The corresponding best-fit

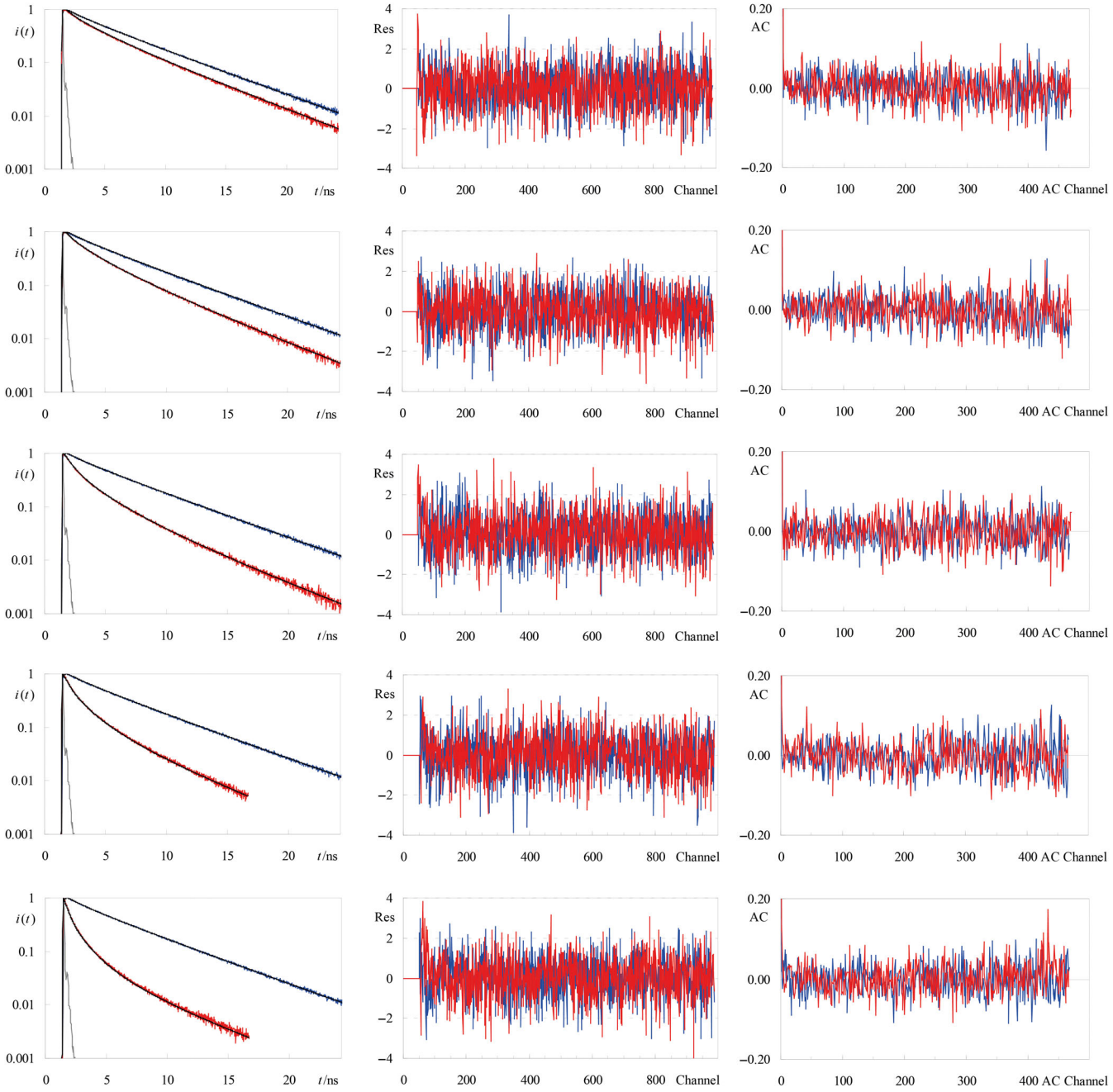

FIGURE 5 Fluorescence intensity decays of Marina Blue SP-C in POPC membranes in the presence of unlabeled or BODIPY-labeled SP-C. Fluorescence intensity decays of Marina Blue SP-C (5 μM) in POPC vesicles (1 mM), in the presence of unlabeled SP-C (blue lines) or BODIPY SP-C (red lines), of concentration (either unlabeled or labeled with BODIPY), from top to bottom: 1.25, 2.5, 5, 7.5, and 15 μM. In the left panels, the fitting curves (Equations (9)–(11)) to each data set and the instrumental response function are also shown (in black and gray, respectively). The middle and right plots in each row show the residuals and residual auto-correlation plots for the corresponding concentration of unlabeled (blue) or BODIPY-labeled (red) SP-C.

parameters are given in Table 3, while the ones for the Marina Blue rSP-C/BODIPY rSP-C FRET pair are shown in Table 4.

While both the fitted curves of Figure 5 and the fitting parameters in Tables 3, 4 concern the analysis of the ongoing hetero-FRET between the MB- and BODIPY-labeled proteins within the framework of Equations (9)–(11) (with two non-equivalent populations of labeled protein), it should be noted that, for both the fluorescently-labeled SP-C and rSP-C in POPC, the decays of the most dilute samples could be successfully analyzed with a simple formalism, considering a single population. This is clear in the approximately equal c_1 and c_2 values obtained for [BODIPY SP-C] = 2.5 μM

TABLE 3 Time-resolved fluorescence data from FRET between Marina Blue SP-C and BODIPY SP-C in POPC membranes.

[BODIPY SP-C]/μM	1.25	2.5	5	7.5	15
Freely adjusted c_1 and c_2 parameters					
Recovered c_1/ns^{-3}	0.161	0.280	0.606	0.842	1.206
Recovered c_2/ns^{-3}	2.594	0.279	0.024	0.088	0.000
Recovered q	0.0297	0.856	0.0565	0.0732	0.0264
Calculated $<c>$/ns^{-3} (Equation (13))	0.23	0.28	0.57	0.79	1.18
Global χ^2 (considering both donor-only and donor-plus-acceptor decay for each [BODIPY SP-C])	1.11	1.06	1.28	1.27	1.20
Fixed $c_2 = 0$					
Recovered c_1/ns^{-3}	0.162	0.280	0.601	0.811	1.206
Recovered q	0.000	0.000	0.0488	0.0459	0.0264
Calculated $<c>$/ns^{-3} (Equation (13))	0.16	0.28	0.57	0.78	1.18
Global χ^2 (considering both donor-only and donor-plus-acceptor decay for each [BODIPY SP-C])	1.11	1.06	1.28	1.27	1.20

Note: Data obtained from plots in Figure 5.

TABLE 4 Time-resolved fluorescence data of FRET between Marina Blue rSP-C and BODIPY rSP-C in POPC membranes.

[BODIPY rSP-C]/μM	1.25	2.5	5	7.5	15
Freely adjusted c_1 and c_2 parameters					
Recovered c_1/ns^{-3}	0.089	0.178	0.290	0.262	0.367
Recovered c_2/ns^{-3}	0.089	0.178	0.290	0.520	1.024
Recovered q	0.773	0.867	2.14	2.16	0.927
Calculated $<c>$/ns^{-3} (Equation (13))	0.089	0.18	0.29	0.44	0.68
Global χ^2 (considering both donor-only and donor-plus-acceptor decay for each [BODIPY rSP-C])	1.06	1.27	1.35	0.97	1.18
Fixed $c_2 = 0$					
Recovered c_1/ns^{-3}	0.089	0.178	0.290	0.441	0.611
Recovered q	0.000	0.000	0.000	0.0324	0.0571
Calculated $<c>$/ns^{-3} (Equation (13))	0.09	0.18	0.29	0.43	0.58
Global χ^2 (considering both donor-only and donor-plus-acceptor decay for each [BODIPY rSP-C])	1.06	1.27	1.35	0.98	1.24

(Table 3; even though this is not the case for 1.25 μM, consideration of a single population would lead to an identically good fit, with $c = 0.162$ ns^{-3} and global $\chi^2 = 1.11$) and [BODIPY rSP-C] = 1.25, 2.5, and 5 μM (Table 4). However, using higher acceptor concentrations leads to donor fluorescence intensity decays that can only be successfully analyzed by allowing for a second population. For fluorescently labeled SP-C (Table 3), this is apparent in a small (<8%) fraction of isolated donors, that is, reporting a decreased local concentration of acceptors ($c_2 << c_1$). We believe that this result is not very significant, since the calculated average concentration, $<c>$, remains close to the c_1 value; the residual c_2 component could arise from an imperfect linkage of the donor and acceptor decay samples. Significantly, when c_2 is fixed to zero, the quality of the global fits is not affected, and the recovered isolated donor fractions are consistently <5%.

To some extent, this situation is also verified for rSP-C (Table 4). However, somewhat differently for the highest concentrations, when both c_1 and c_2 are optimized, their recovered values are finite, differing by a factor of 2–3, with comparable amplitudes (q is neither very small nor very large, indicating significant contributions of both populations), which points to a slightly more heterogeneous population. This result would be expected for a phase-separated lipid system, with two coexisting phases, with differences in distribution of donor- and

acceptor-labeled proteins according to their respective preferences. This is actually what is observed for the Marina Blue SP-C/BODIPY SP-C FRET pair in the LM and LS systems, where two populations of donors are inferred, one sensing acceptor depletion ($0.1\ ns^{-3} < c_1 < 0.4\ ns^{-3}$), while the other reports a local higher acceptor concentration ($1.5\ ns^{-3} < c_2 < 3.6\ ns^{-3}$), compatible with a partition coefficient of acceptor between these two phases of c_2/c_1 (Loura & Prieto, 2000) ≅10 (see Tables S1 and S2). In fact, in the case of fluorescently labeled SP-C in these more complex membrane systems, composed of both unsaturated and saturated phospholipids and (in the case of LS) cholesterol, an underlying heterogeneous lipid organization is expected. This is not the case for rSP-C in single-component POPC membranes, where the recovery of two distinct and significant populations can only be interpreted as a non-homogeneous distribution of protein at high concentrations, with possible coexistence of monomers and aggregates, which would account for the lower and higher c values, respectively.

From Equation (13), a linear dependence of c on the analytical acceptor surface concentration n is expected. n (molecules/Å^2) can be readily calculated from the probe:lipid ratio divided by the lipid molecular area (taken as 66 Å^2 for POPC; Filipe et al., 2015), and used to obtain theoretical estimates of c. The latter are compared with the <c> values recovered from the decay fits of Marina Blue SP-C and rSP-C in POPC (Figure 6). Taking into account that the theoretical line in Figure 6A is not a fit (but the direct result of applying Equation (13) with independently obtained parameters), there is good agreement between the theoretical line and the recovered <c> values for SP-C, with linear dependence of the latter on protein concentration being kept up to 7.5 μM (or lipid:protein = 133). Deviations from the theoretical line may stem from several factors, including uncertainty in absolute lipid or protein concentrations, as well as lipid molecular area. Only for very high protein concentration (15 μM, or lipid:protein = 67) a clear deviation from linearity to <c> lower values becomes apparent, probably indicating onset of aggregation. Similar behaviors were observed for this protein in the other lipid systems (Figure S1). In contrast, for rSP-C in POPC, this deviation occurs at lower concentrations, pointing to higher propensity for protein aggregation.

While the fitting of FRET models to the decays provides important clues regarding the organization of SP-C and rSP-C in the different lipid systems, a simpler, more immediate, and model-independent analysis may be carried out by comparing the FRET efficiencies obtained from time-resolved data, using amplitude averaged lifetimes $\overline{\tau}$ (Equation (2)),

$$E_{TR} = 1 - \overline{\tau}_{DA}/\overline{\tau}_{D}, \tag{14}$$

with those determined, in the same samples, from steady-state measurements, using fluorescence intensities I:

$$E_{ss} = 1 - I_{DA}/I_{D}. \tag{15}$$

In both equations, "D" and "DA" denote the donor-only and the donor + acceptor samples, respectively. The presence of donor–acceptor aggregation would give rise to donors quenched with 100% efficiency, invisible in the time-resolved experiment, but whose lack of emission would be reflected in a reduced I_{DA} in the steady-state measurement. This situation would, in turn, be manifested as $E_{SS} > E_{TR}$. Conversely, the absence of a

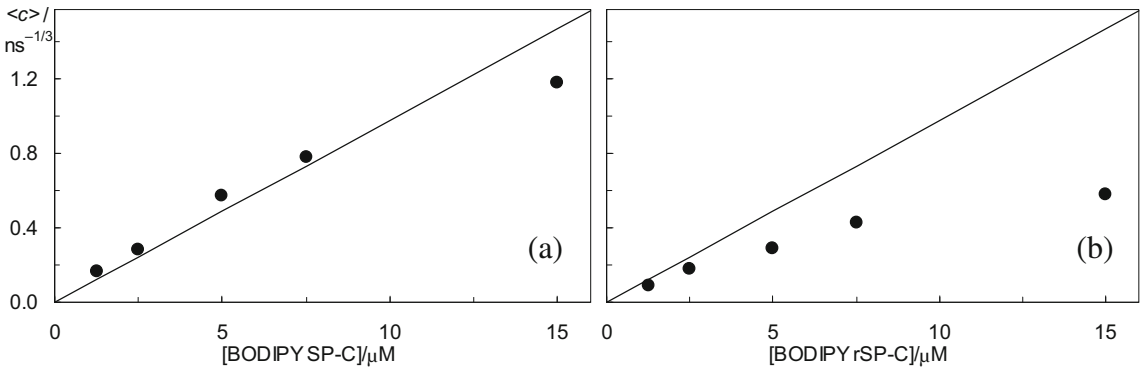

FIGURE 6 Overall surface acceptor concentrations as a function of protein content as determined by FRET data. Overall acceptor concentrations <c> (circles) recovered from fitting Equations (9)–(11) to the time-resolved FRET data, with fixed $c_2 = 0$. (a) fluorescently labeled SP-C in POPC (Figure 5, Table 3); b: fluorescently labeled rSP-C in POPC (Table 4). The lines are the theoretical values calculated from the actual acceptor concentrations with Equation (13) (straight line), using the spectroscopic $R_0 = 4.93$ nm value, and an area/POPC lipid molecule = 0.66 nm^2 (Filipe et al., 2015).

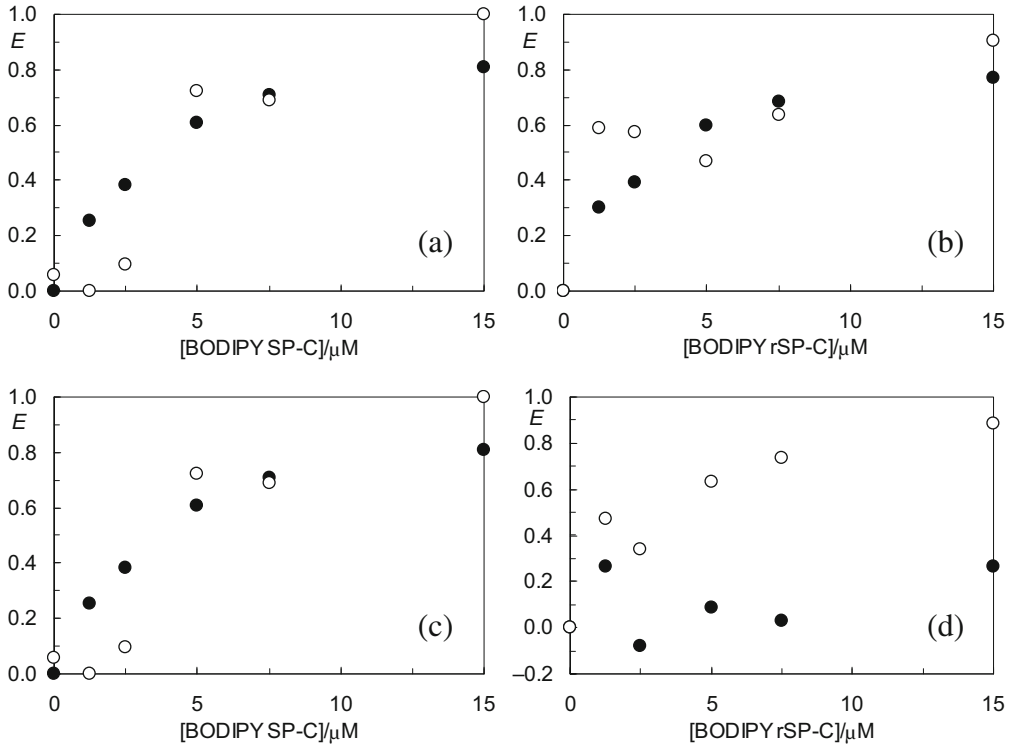

FIGURE 7 FRET efficiencies from Marine Blue SP-C to BODIPY SP-C or rSP-C as calculated from time resolved and steady-state fluorescence. FRET efficiency E calculated from time-resolved (E_{TR}; filled circles) or steady-state (E_{SS}; open circles) fluorescence experiments with Marine Blue SP-C/BODIPY SP-C (a,c) or Marina Blue rSP-C/BODIPY rSP-C (b,d) donor–acceptor pairs, are compared in the plots, in POPC (a,b) or LS (c,d) membrane systems.

systematic order relation between E_{SS} and E_{TR} would point to absence of extensive donor–acceptor (and thus protein) aggregation.

Analysis of Figure 7 reveals a monotonic variation of E_{TR}, except for rSPC in LS (Figure 7D), while data for E_{SS} is largely scattered. This is unsurprising, since the latter depends critically on donor concentration, which is an additional cause of experimental uncertainty. Still, it can be safely concluded that in both POPC and LS membrane systems, the variations of E_{SS} and E_{TR} for the SP-C-based FRET pair have a similar trend of variation (Figures 7A,C). This is not the case for the rSP-C-based FRET pair. In POPC, E_{SS} and E_{TR} are close, and only at lower acceptor concentrations the higher E_{SS} points out to some extent of static quenching of Marina Blue rSP-C by BODIPY rSP-C, likely caused by aggregation. On the other hand, for LS (Figure 7D), E_{TR} displays an erratic dependence on acceptor concentration, around low values, denoting inefficient FRET. This contrasts with the corresponding E_{SS} variation, which shows the expected sublinear increase to values close to unity for high acceptor concentration. This behavior can be interpreted as extensive static quenching of most donor fluorophores by acceptors, indicative of aggregation. The TR data reflect that the "surviving" donors, probably monomers segregated from the quenched aggregates, reside mostly in an acceptor-deprived microenvironment, and FRET from them is inefficient.

3 | DISCUSSION

The homodimerization of SP-C has been investigated in previous in silico or experimental studies, in which the full sequence or the structure of the studied protein were slightly different to that of native SP-C (Barriga et al., 2021; Kairys et al., 2004; Korolainen et al., 2022; Wang et al., 2002). In the present work, through a combination of fluorescence self-quenching and hetero-FRET studies we were able to evaluate the interplay between the palmitoylation state of SP-C and the lateral organization of the lipid membranes on the aggregation state and membrane compartmentalization of the protein. For this purpose, three different membrane mimetic systems were explored: (i) POPC membranes, in an entirely fluid disordered state; (ii) DPPC/POPC/POPG (50:25:15 w/w/w) mixed membranes, somehow mimicking in a simplified version the lipid composition of pulmonary surfactant and a likely coexistence of disordered and ordered phases, and (iii) membranes made of full lipid surfactant (LS) directly extracted from native pulmonary surfactant. This complex mixture comprises mainly DPPC, other phospholipids as phosphatidylglycerol phosphatidylinositol and phosphatidylserine, smaller amounts of other phospholipids, and neutral lipids such as cholesterol.

It had been proposed that SP-C could be able to interact with another molecule of SP-C through the extremely conserved AxxxG motif contained at the end of its α-helix

(Kairys et al., 2004) or through the PCCP sequence located at its N-terminal (Plasencia et al., 2004). However, our analysis from fluorescence intensities obtained during steady-state self-quenching assays reveals that SP-C does not apparently oligomerize within fluid POPC membranes, where compartmentalization is not possible. This result is consistent with the data obtained by Horowitz and collaborators (Horowitz et al., 1993). They studied Förster resonance energy transfer between NBD-labeled SP-C and Eoisin 5-isothiocyanate (EITC) SP-C into DPPC:DMPG (7:1) membranes at different temperatures. When the temperatures were higher than the melting temperature of the membranes, the observed extent of FRET was compatible with a uniform distribution of the protein. This points out that SP-C does not dimerize if there is no lipid phase separation on the system under study. We have also studied here the oligomerization state of SP-C in membranes whose composition emulates the lipid composition of PS (LM) and in membranes with the full lipid complexity of PS, here called LS. An important difference between them is the presence of cholesterol, only present in LS, where it regulates the fluidity of segregated ordered-like membrane domains (Doole et al., 2022). Concerning LM membranes, our results from self-quenching assays using just BODIPY SP-C are similar to those obtained in POPC membranes. Still, two populations of donors were determined (Table S1) indicating that SP-C could be compartmentalized. A similar situation occurs in LS membranes, in which the high apparent diffusion coefficient obtained in this study corroborates our previous observation of fast collisional quenching of wildtype SP-B by wildtype SP-C in the same lipid system (Kang et al., 2022). In addition, dimerization constants deduced from steady-state self-quenching in LS membranes seem to point out that monomers of SP-C might exhibit very little aggregation. Research performed by Horowitz et al. (1993) at temperatures below phase transition in different synthetic lipid systems revealed an increased extent of energy transfer between NBD SP-C and EITC SP-C. However, they could not distinguish between true protein oligomerization and the possible existence of membrane patches enriched in SP-C as a mere consequence of the phase separation, due to the lower sensibility of the equipment used. Considering all these studies, one can conclude that SP-C is likely mainly monomeric, although it is able to form a small amount of dimers if there is a significant lipid phase separation. Some simulation studies have suggested that SP-C could form dimers, but they were performed taking into account just the α-helical segment of SP-C (Kairys et al., 2004) or the entire molecule of SP-C without palmitoylation (Korolainen et al., 2022). In the current study, we have carried out experiments to analyze potential protein oligomerization of a non-palmitoylated recombinant human version of SP-C(rSP-C) expressed in bacteria, lacking the palmitoylation machinery.

The structure and properties of this recombinant version were studied in detail by Baumgart et al. (2010). It has been suggested that palmitic acids of native SP-C could promote a deeper insertion of the N-terminal segment of the protein into membrane layers and a decrease in the degree of tilting of the protein in lipid bilayers (Roldan et al., 2015). As a consequence, rSP-C would have different restrictions in the geometry of the protein into the membrane, leading to the possible formation of a higher proportion of dimers than native SP-C. Alternatively, a partial mismatch of the less tilted protein with respect to the membrane thickness could promote an enhanced protein segregation from the lipids, thus favoring protein–protein associations.

All parameters obtained indicate that rSP-C could form dimers even in POPC membranes. The lateral diffusion coefficient calculated from Stern–Vomer equation is higher than determined for the palmitoylated BODIPY-labeled SP-C in POPC membranes (Table 2). Steady state self-quenching of rSP-C in POPC membranes demonstrated the existence of aggregation, with a dimerization constant higher than that found for SP-C in LS membranes. Therefore, we conclude that there are more dimers of rSP-C in POPC membranes than dimers of SP-C in LS, where there is a pronounced phase segregation. In addition, according to time resolved FRET parameters (Figure 6), the concentration of rSP-C required for aggregation is smaller than the corresponding concentration of SP-C. This is consistent with the study of a dimeric form of a recombinant mutant protein, rSP-C (FFI), in chloroform/methanol solutions using high resolution NMR spectroscopy (Johansson et al., 1994). To investigate the influence of phase separation, where rSP-C molecules would be closer due to compartmentalization, LM and LS systems were used. In both systems, the presence of dimers is higher in rSP-C than in POPC membranes (Table 5). The lateral diffusion coefficient obtained from Stern–Volmer equation for BODIPY rSP-C in LS membranes is larger than that in LM system, potentially indicating a greater segregation of lipid domains, a facilitated interaction between monomers of rSP-C, or a combination of both processes. According to the SP-C state determined in the three lipid systems studied here, the membranes of LS could be the most compartmentalized. Therefore, it would be expected that the formation of rSP-C dimers would be particularly promoted in LS membranes. In contrast, the concentration of rSP-C required for protein–protein interaction is the lowest in LM (Table 5). This suggests that phase separation promotes oligomerization, but it might not

TABLE 5 Evidences from fluorescence experiments regarding the oligomeric state of SP-C.

Lipid system	SP-C	rSP-C
POPC	• *Self-quenching*: diffusion similar to host lipid, no evidence for aggregation. • *FRET*: essentially uniform distribution. Small (<5%) fraction of isolated labeled protein for higher concentrations (L/P < 200).	• *Self-quenching*: two-fold faster apparent diffusion compared to SP-C. Static quenching indicates slight evidence for aggregation at high concentrations (∼8% protein dimerized at L/P = 100). • *FRET*: essentially uniform distribution for low concentrations. Heterogeneous distribution for L/P < 200: two donor populations with two- to three-fold differences in local acceptor concentration.
LM (DPPC/POPC/POPG lipid mixture)	• *Self-quenching*: diffusion similar to POPC, no evidence for aggregation. • *FRET*: protein distribution in two different environments, with local concentrations differing by ∼1 order of magnitude, underlying lipid phase coexistence	• *Self-quenching*: faster apparent diffusion, by 1 order of magnitude compared to POPC, compatible with compartmentalization. Static quenching indicates clear aggregation, with ∼50% protein dimerized at L/P = 500.
LS (Lipid Surfactant)	• *Self-quenching*: faster apparent diffusion, by 1 order of magnitude compared to the same protein in POPC and LM, compatible with compartmentalization. However, no evidence for aggregation from steady-state data, apart from statistical contacts. • *FRET*: protein distribution in two different environments, with local concentrations differing by ∼1 order of magnitude, underlying lipid phase coexistence	• *Self-quenching*: faster apparent diffusion, by 1 order of magnitude compared to POPC compatible with compartmentalization. Static quenching indicates clear aggregation, with ∼50% protein dimerized at L/P = 200. • *FRET*: efficient donor quenching detected in steady-state data, virtually undetectable in time-resolved conditions (formation of highly quenched aggregates, leaving "surviving" fluorophores isolated).

exclusively depend on the degree of compartmentalization but on the nature of the segregated phases, or possible defined protein/lipid interactions, among other possible factors.

The main structural difference between rSP-C and SP-C is the palmitoylation state. Considering the degree of aggregation detected in POPC membranes, it seems that palmitoylation could prevent, at least partially, the interaction among SP-C monomers. Our results suggest that rSP-C could tend to form more dimers than SP-C, for which dimerization could not be completely established. Despite of this, dimers of native palmitoylated SP-C have been observed, in a minimal proportion, during purification of this protein in different species, such as bovine, canine, porcine, or rat SP-C (Baatz et al., 1992; Creuwels et al., 1995; Luy et al., 2004; Wang et al., 2002). The secondary structure proposed for the SP-C preparations analyzed in those studies were β-sheet for the bovine protein and α-helical for the canine protein. Thus, one could expect that the amino acids implied in the formation of the possible homodimers would be different depending on the protein secondary structure. In Baatz and collaborators' assays (Baatz et al., 1992), the yielding of fatty acids liberated upon deacylation was lower in SP-C dimers, pointing out that the cysteines in the PCCP motif within the N-terminal segment of SP-C could participate in intermolecular disulfide bonds. Whether the potential formation of intermolecular disulfides precedes or is rather a consequence of protein dimerization/oligomerization, remains to be established. Regarding the formation of dimers in α-helical canine SP-C, it was observed in a non-acylated form of 7 kDa, indicating again the generation of a dimer through intermolecular disulfide biding of PCCP motif as defined in Creuwels et al. (1995). In NMR studies with porcine SP-C, two sets of resonances were resolved at the C-terminal segment of the protein, suggesting the potential coexistence of monomers and dimers (Johansson et al., 1994). Because of that, Luy et al. investigated a recombinant mutant of human SP-C shifting the PCCP sequence to PFFI (Luy et al., 2004). That work supported the three-state model proposed previously for SP-C (Szyperski et al., 1998): (1) monomeric α-helix, (2) dimeric α-helix, and (3) β-sheet fibrils. Such dimeric α-helix structure would not be formed through disulfide bonds due to the absence of cysteines in the sequence of mutant rSP-C (FFI). This interaction could be performed through hydrogen bonds or Van der Waals forces implying the AxxxG motif or the recently proposed region V21xxxVxxxGxxxM33 (Kairys et al., 2004; Korolainen et al., 2022). All these studies

seem to suggest a connection between SP-C depalmitoylation and the formation of dimers/oligomers. Our results in the present study indicate that, beyond the potential formation of disulfide bonds, the lack of palmitic chains at the N-terminal moiety of the SP-C structure could be a factor promoting by itself protein–protein interactions and the stabilization of higher order oligomers.

FRET studies performed in this work could not determine the secondary structure of SP-C dimers/oligomers. Currently, the physiological implication of dimerization is not defined. SP-C dimer adopting an α-helix structure could be embedded in the membrane bilayer in an analogous fashion to the monomer, and would be able to achieve the insertion of phospholipids into the interfacial monolayer as well as SP-C monomers, with a slight difference in the kinetics (Creuwels et al., 1995). It has been hypothesized that SP-C dimers might adopt a rigid transmembrane V-shaped structure that would trigger membrane fragmentation (Roldan et al., 2016). Recently, Korolainen et al. have proposed three plausible different structures for non-palmitoylated SP-C homodimers according with its stability or lowest free energy calculated from MD simulations: (1) parallel dimer; (2) inverted V-shape dimer, and (3) V-shape dimer (Korolainen et al., 2022). Our results from rSP-C self-quenching would imply the formation of rSP-C dimers but considering the distance between the N-terminal end of the molecules of rSP-C in the inverted V-shape topology, this structure seems improbable. The most compatible conformation would be the parallel dimer, although the V-shape dimer cannot be discarded. Vesicles possibly produced by SP-C-promoted membrane fission could be endocytosed by alveolar macrophages or AT2 cells (Barriga et al., 2021; Sehlmeyer et al., 2020). In this way, α-helical stable or transient SP-C dimers could participate in processing and homeostasis of different fractions of surfactant in the alveoli. The results from the current work suggest that dimerization of SP-C could be minimal and would depend on phase separation and protein concentration (Table 5). However, during breathing, local lipid composition, as well as compartmentalization degree and SP-C concentration, is constantly changing in both membranes and interfacial multilayered films of surfactant (Keating et al., 2012; Pastrana-Rios et al., 1994). Conversely to α-helix SP-C dimers, the functional behavior of those with a β-sheet structure functions has not been characterized in detail. It has been proposed that they could end forming a β-barrel, similar to some transmembrane proteins such as porin, affecting the lipid transference between bilayers and monolayers during breathing-like compression-expansion dynamics (Baatz et al., 1992).

Previously, the transition from an α-helical SP-C monomer to a protein form with β-sheet conformation has been observed (Cruz et al., 1995; Szyperski et al., 1998; Wüstneck et al., 2003). Fibrillogenic amyloid-like aggregates produced by the accumulation of β-sheet strands are related to pathologies as pulmonary fibrosis and alveolar proteinosis (Beers & Mulugeta, 2005; Johansson, 2001; Johansson et al., 2004). The BRICHOS sequence contained within the precursor of SP-C (proSP-C) is a chaperone domain that promotes α-helix structure and stabilizes it until palmitoylation of the protein occurs (Gustafsson et al., 2001; Johansson et al., 2009; Sánchez-Pulido et al., 2002). All this seems to indicate that in absence of this domain, the β-sheet structure that could be eventually formed would be an anomalous, potentially pathogenic, conformation.

In conclusion, the results of this work suggest that palmitoylation could be important to stabilize the monomeric α-helical conformation of SP-C, which is likely optimal to perform the role of the protein to stabilize the interfacial surfactant films along the demanding breathing dynamics. Eventual depalmitoylation as a consequence of lung injury and oxidation, accumulation of the protein to high densities because of membrane compartmentalization and other potential factors could end in the extensive formation of protein dimers and other possible higher order oligomers that could affect function to extents that need to be analyzed in detail and that could be associated with certain pathogenic situations. It has been proposed that protein oligomerization could be associated with membrane remodeling and the fragmentation of surfactant layers into small vesicles enriched in SP-C, which could thus be prone to uptake by alveolar macrophages or alveolar pneumocytes. The palmitoylation state of SP-C could then serve as part of the sensors triggering surfactant recycling, the metabolism that maintains alveolar homeostasis.

4 | MATERIALS AND METHODS

4.1 | Materials

All synthetic lipids were purchased from Avanti Polar Lipids (Alabaster, AL). The lung surfactant lipid fraction (LS) was isolated from lavages with Tris buffer (5 mM Tris 150 mM NaCl pH 7.0) of porcine lungs. After isolation of lipid–protein complexes by ultracentrifugation (31,000 rpm, 1 h, 4°C; HIMAC CP100NX), PS was purified by density gradient centrifugation as described previously (Taeusch et al., 2005). The hydrophobic components of PS were collected by performing an

organic extraction (Bligh & Dyer, 1959) and chromatographed using a Sephadex LH-20 resin equilibrated with chloroform/methanol (2:1, v/v) to separate LS from the hydrophobic proteins. LS fraction was quantified for phosphorous content (Rouser et al., 1970).

The organic extract containing the two hydrophobic surfactant proteins (SP-B and SP-C), was obtained from minced porcine lungs according to the Bligh and Dyer method (Bligh & Dyer, 1959). It was then loaded onto a Sephadex LH-20 (GE, Healthcare) chromatography column equilibrated with chloroform/methanol (2:1, v/v) from Merck (Darmstadt, Germany). Finally, SP-B and SP-C contained within the protein fraction resulting from this chromatography were isolated using a Sephadex LH-60 resin equilibrated with chloroform/methanol (1:1, v/v) acidified with a 0.5% volume of HCl (0.1 N).

Non palmitoylated recombinant SP-C (rSP-C) was purified following the protocol of Lukovic et al. (2006) with changes as described by Roldan et al. (2015). The sequence of rSP-C is GPFGIPCCPVHLKRLLIVVVVVVLI VVVIVGALLMGL, including an extension of two additional amino acids at the N-terminal end with respect to the sequence of human SP-C, as a consequence of the production and purification procedure. This extension had no significant effect on the interfacial activities of the protein as assessed previously (Lukovic et al., 2006). Protein concentration was quantified by amino acid analysis.

4.2 | Protein labeling

The N-terminal end of SP-C or rSP-C was labeled with BODIPY-FL NHS ester (D2184, Invitrogen, ThermoFisher Scientific) or Marina Blue® NHS ester (1242-5, Fluoroprobes) probes as described (Cabre et al., 2018) with some modifications. For all labeling reactions except for rSP-C conjugated with Marina Blue, the apparent pH of both pure proteins in the organic solvent (chloroform/methanol, 1:1, v/v) was adjusted to 7.1 with the appropriate amount of 50 mM Tris in methanol. To label rSP-C with Marina Blue, the solution containing pure rSP-C was slightly alkalinized (pH 7.5). Then, the required probe was incubated overnight at 4°C with pure proteins in a 5:1 probe/protein molar ratio. The labeling procedure was stopped by decreasing the apparent pH to 2 with HCl. Finally, the samples were loaded onto a Sephadex LH-20 resin equilibrated with chloroform/methanol (1:1, v/v) acidified with a 0.5% of HCl (0.1 N) to separate the labeled protein from free probe. Protein concentration was finally quantified by amino acid analysis.

The amount of dye conjugated to each protein was calculated using the Lambert–Beer law where the molar extinction coefficients (ε) used were $\varepsilon_{504nm} = 82 \times 10^3$ $M^{-1}\,cm^{-1}$ for BODIPY-FL and $\varepsilon_{365nm} = 19 \times 10^3$ $M^{-1}\,cm^{-1}$ for Marina Blue (Haugland, 2002). The final dye:protein molar ratios (D/P) determined for the fluorescently-labeled proteins were D/P = 0.5 for BODIPY-FL/SP-C, D/P = 0.8 for BODIPY-FL/rSP-C, D/P = 0.5 for Marina Blue/SP-C, and D/P = 0.7 for Marina Blue/rSP-C, respectively.

To check whether the introduction of the fluorescent probes could alter protein conformation, we obtained the circular dichroism (CD) spectra of the different proteins reconstituted in micelles of lysophosphatidylcholine (LPC). In brief, proper amounts of each protein and LPC were dried in a 1:7 mass ratio under a stream of nitrogen and then under vacuum for 2 h and samples were resuspended in PBS (4.4 mM KH_2PO_4, 5.6 mM Na_2HPO_4, 50 mM NaCl, pH 6.8) through five cycles of freeze with liquid nitrogen and thaw at 25°C, vortexing 30 s between each cycle. Quartz cells of 0.1 cm optical path were used to record the CD spectra in a JASCO J-715 Circular Dichroism CD Spectrometer at 25°C. Data analysis was performed with Spectra Manager Software and the BestSel™ online tool was used to achieve CD deconvolution. All the CD spectra were consistent with a mainly alpha-helical conformation for all the protein forms studied, palmitoylated and non-palmitoylated, with and without fluorescent groups attached.

4.3 | Preparation of multilamellar vesicles (MLVs)

Three lipid systems were used: (1) 1-palmitoyl-2-oleoyl-*sn*-glycero-3-phosphocholine (POPC); (2) a synthetic lipid mixture (LM) composed of DPPC (1,2-dipalmitoyl-*sn*-glycero-3-phosphocholine), POPC and POPG (1-palmitoyl-2-oleoyl-*sn*-glycero-3-phosphoglycerol) (50/25/15, w/w/w), and (3) the surfactant lipid fraction (LS) obtained from native PS.

Lipid and lipid/protein MLV samples were prepared by co-drying a proper amount of lipid and fluorescently-labeled protein under a stream of nitrogen that was finally subjected to vacuum during 2 h. The dried lipid or lipid/protein samples were then suspended in 5 mM Tris, 150 mM NaCl pH 7 at 45°C, frozen with liquid nitrogen, and thawed in a bath at 45°C. Five freeze/thaw cycles were performed with vortexing between each cycle to obtain the desired MLVs (Traïkia et al., 2000).

For the fluorescence self-quenching assays, variable concentrations of BODIPY SP-C or BODIPY rSP-C (namely 1.25, 2, 3.5, 5, and 7.5 μM in reference to the fluorophore concentration) were co-solubilized with 1 mM of the desired lipids in order to obtain the

fluorescently-labeled protein-loaded MLVs. For the hetero-Förster Resonance Energy Transfer (FRET) studies, the systems used were similar to the self-quenching assays. However, in this case, a FRET donor, Marina Blue SP-C or Marina Blue rSP-C (5 μM of fluorescently-labeled protein), was also added to prepare the protein-containing MLVs.

4.4 | Fluorescence spectroscopy

The fluorescence self-quenching and hetero-FRET studies were carried out by performing both steady-state and time-resolved fluorescence measurements of the MLVs containing variable surface concentrations of the fluorescently-labeled native and recombinant SP-C protein. Steady-state measurements were acquired with a Horiba-Jobin Yvon Fluorolog 3-22 (Tokyo, Japan) spectrofluorimeter, using 0.5 × 0.5 cm quartz cuvettes. For the time-resolved fluorescence measurements, a time-correlated single-photon timing system was used. Excitation of Marina Blue and BODIPY-labeled proteins was carried out at 340 nm (using the second harmonic of a secondary dye laser of DCM from Coherent DCM 700 series), and 488 nm (using a ps laser diode from Becker & Hickl [Berlin, Germany] series BPS-488-SM), respectively, whereas emission from MB- and BODIPY-labeled proteins was recorded at 455m and 515 nm, respectively. Data analysis was carried out using the TRFA data processor Advanced Version 1.4 from Scientific Software Technologies Center (Belarusian State University, Minsk) (Marquardt, 1963). The goodness of the fits was judged from the experimental χ^2 value ($\chi^2 < 1.5$ indicating adequate fitting), weighted residuals and autocorrelation plots.

AUTHOR CONTRIBUTIONS

Begoña García-Álvarez: Conceptualization; investigation; funding acquisition; writing – original draft; methodology; validation; visualization; writing – review and editing; project administration; data curation; supervision; resources. **Mishelle Morán-Lalangui:** Conceptualization; investigation; writing – original draft; methodology; visualization; writing – review and editing; software; formal analysis; data curation; validation. **Ana Coutinho:** Conceptualization; investigation; writing – review and editing; writing – original draft; methodology; validation; visualization; software; formal analysis; supervision; data curation. **Manuel Prieto:** Funding acquisition; conceptualization; validation; writing – original draft; writing – review and editing; project administration; supervision; data curation; investigation; visualization; methodology; resources. **Alexander Fedorov:** Methodology; investigation; visualization. **Jesús Pérez-Gil:** Conceptualization; investigation; funding acquisition; writing – original draft; validation; writing – review and editing; project administration; supervision; resources; data curation. **Luís M. S. Loura:** Formal analysis; software; conceptualization; investigation; writing – original draft; methodology; validation; visualization; writing – review and editing; supervision; data curation; resources.

ACKNOWLEDGMENTS

Begoña García-Álvarez and Jesús Pérez-Gil thanks Spanish Ministry of Science and Innovation Grant (PID2021-124932OB-100) and Community of Madrid Grant (Nanobiocargo P2018/NMT-4389) for funding this study. Mishelle Morán-Lalangui is a recipient of a FPI fellowship from the Spanish Ministry of Science and Innovation. Luís M. S. Loura acknowledges funding by the European Regional Development Fund, through COMPETE2020-Operational Program for Competitiveness and Internationalization, and Portuguese funds via FCT-Fundação para a Ciência e a Tecnologia, under projects UIDB/00313/2020 and UIDP/00313/2020 (Portugal). Ana Coutinho and Manuel Prieto acknowledge funding from FCT-Fundação para a Ciência e a Tecnologia, under projects UIDB/04565/2020, UIDP/04565/2020 and LA/P/0140/2020 (Portugal). This work has been supported by a working visit bursary from EBSA.

CONFLICT OF INTEREST STATEMENT

The authors declare no competing interests.

ORCID

Begoña García-Álvarez https://orcid.org/0000-0003-3774-1999

REFERENCES

Amin RS, Wert SE, Baughman RP, Tomashefski JF Jr, Nogee LM, Brody AS, et al. Surfactant protein deficiency in familial interstitial lung disease. J Pediatr. 2001;139:85–92. https://doi.org/10.1067/mpd.2001.114545

Ariki S, Nishitani C, Kuroki Y. Diverse functions of pulmonary collectins in host defense of the lung. J Biomed Biotechnol. 2012; 2012:532071. https://doi.org/10.1155/2012/532071

Augusto L, Le Blay K, Auger G, Blanot D, Chaby R. Interaction of bacterial lipopolysaccharide with mouse surfactant protein C inserted into lipid vesicles. Am J Physiol Lung Cell Mol Physiol. 2001;281:L776–85. https://doi.org/10.1152/ajplung.2001.281.4.L776

Augusto LA, Li J, Synguelakis M, Johansson J, Chaby R. Structural basis for interactions between lung surfactant protein C and bacterial lipopolysaccharide. J Biol Chem. 2002;277:23484–92. https://doi.org/10.1074/jbc.M111925200

Augusto LA, Synguelakis M, Espinassous Q, Lepoivre M, Johansson J, Chaby R. Cellular antiendotoxin activities of lung surfactant protein C in lipid vesicles. Am J Respir Crit Care

Med. 2003;168:335–41. https://doi.org/10.1164/rccm.200212-1440OC

Augusto LA, Synguelakis M, Johansson J, Pedron T, Girard R, Chaby R. Interaction of pulmonary surfactant protein C with CD14 and lipopolysaccharide. Infect Immun. 2003;71:61–7. https://doi.org/10.1128/IAI.71.1.61-67.2003

Baatz JE, Smyth KL, Whitsett JA, Baxter C, Absolom DR. Structure and functions of a dimeric form of surfactant protein SP-C: a Fourier transform infrared and surfactometry study. Chem Phys Lipids. 1992;63:91–104. https://doi.org/10.1016/0009-3084(92)90026-l

Barriga A, Moran-Lalangui M, Castillo-Sanchez JC, Mingarro I, Perez-Gil J, Garcia-Alvarez B. Role of pulmonary surfactant protein Sp-C dimerization on membrane fragmentation: an emergent mechanism involved in lung defense and homeostasis. Biochim Biophys Acta Biomembr. 2021;1863:183572. https://doi.org/10.1016/j.bbamem.2021.183572

Baumgart F, Ospina OL, Mingarro I, Rodríguez-Crespo I, Pérez-Gil J. Palmitoylation of pulmonary surfactant protein SP-C is critical for its functional cooperation with SP-B to sustain compression/expansion dynamics in cholesterol-containing surfactant films. Biophys J. 2010;99:3234–43. https://doi.org/10.1016/j.bpj.2010.08.070

Beers MF, Mulugeta S. Surfactant protein C biosynthesis and its emerging role in conformational lung disease. Annu Rev Physiol. 2005;67:663–96. https://doi.org/10.1146/annurev.physiol.67.040403.101937

Bligh EG, Dyer WJ. A rapid method of total lipid extraction and purification. Can J Biochem Physiol. 1959;37:911–7. https://doi.org/10.1139/o59-099

Cabre EJ, Martinez-Calle M, Prieto M, Fedorov A, Olmeda B, Loura LMS, et al. Homo- and hetero-oligomerization of hydrophobic pulmonary surfactant proteins SP-B and SP-C in surfactant phospholipid membranes. J Biol Chem. 2018;293:9399–411. https://doi.org/10.1074/jbc.RA117.000222

Chou PY, Fasman GD. Prediction of the secondary structure of proteins from their amino acid sequence. Adv Enzymol Relat Areas Mol Biol. 1978;47:45–148. https://doi.org/10.1002/9780470122921.ch2

Chroneos ZC, Sever-Chroneos Z, Shepherd VL. Pulmonary surfactant: an immunological perspective. Cell Physiol Biochem. 2010;25:13–26. https://doi.org/10.1159/000272047

Clark JC, Wert SE, Bachurski CJ, Stahlman MT, Stripp BR, Weaver TE, et al. Targeted disruption of the surfactant protein B gene disrupts surfactant homeostasis, causing respiratory failure in newborn mice. Proc Natl Acad Sci U S A. 1995;92:7794–8. https://doi.org/10.1073/pnas.92.17.7794

Creuwels LA, Demel RA, van Golde LM, Haagsman HP. Characterization of a dimeric canine form of surfactant protein C (SP-C). Biochim Biophys Acta. 1995;1254:326–32. https://doi.org/10.1016/0005-2760(94)00195-5

Cruz A, Casals C, Perez-Gil J. Conformational flexibility of pulmonary surfactant proteins SP-B and SP-C, studied in aqueous organic solvents. Biochim Biophys Acta. 1995;1255:68–76. https://doi.org/10.1016/0005-2760(94)00210-p

Daniels CB, Orgeig S. Pulmonary surfactant: the key to the evolution of air breathing. News Physiol Sci. 2003;18:151–7. https://doi.org/10.1152/nips.01438.2003

Davenport L, Dale RE, Bisby RH, Cundall RB. Transverse location of the fluorescent probe 1,6-diphenyl-1,3,5-hexatriene in model lipid bilayer membrane systems by resonance excitation energy transfer. Biochemistry. 1985;24:4097–108. https://doi.org/10.1021/bi00336a044

Dluhy RA, Shanmukh S, Leapard JB, Kruger P, Baatz JE. Deacylated pulmonary surfactant protein SP-C transforms from alpha-helical to amyloid fibril structure via a pH-dependent mechanism: an infrared structural investigation. Biophys J. 2003;85:2417–29. https://doi.org/10.1016/s0006-3495(03)74665-7

Doole FT, Kumarage T, Ashkar R, Brown MF. Cholesterol stiffening of lipid membranes. J Membr Biol. 2022;255:385–405. https://doi.org/10.1007/s00232-022-00263-9

Fernandes F, Loura LM, Prieto M, Koehorst R, Spruijt RB, Hemminga MA. Dependence of M13 major coat protein oligomerization and lateral segregation on bilayer composition. Biophys J. 2003;85:2430–41. https://doi.org/10.1016/s0006-3495(03)74666-9

Filipe HA, Santos LS, Prates Ramalho JP, Moreno MJ, Loura LM. Behaviour of NBD-head group labelled phosphatidylethanolamines in POPC bilayers: a molecular dynamics study. Phys Chem Chem Phys. 2015;17:20066–79. https://doi.org/10.1039/c5cp01596k

Filippov A, Orädd G, Lindblom G. Influence of cholesterol and water content on phospholipid lateral diffusion in bilayers. Langmuir. 2003;19:6397–400. https://doi.org/10.1021/la034222x

Filippov A, Orädd G, Lindblom G. Lipid lateral diffusion in ordered and disordered phases in raft mixtures. Biophys J. 2004;86:891–6. https://doi.org/10.1016/S0006-3495(04)74164-8

Garcia-Verdugo I, Garcia de Paco E, Espinassous Q, Gonzalez-Horta A, Synguelakis M, Kanellopoulos J, et al. Synthetic peptides representing the N-terminal segment of surfactant protein C modulate LPS-stimulated TNF-alpha production by macrophages. Innate Immun. 2009;15:53–62. https://doi.org/10.1177/1753425908100500

Goerke J. Pulmonary surfactant: functions and molecular composition. Biochim Biophys Acta. 1998;1408:79–89. https://doi.org/10.1016/s0925-4439(98)00060-x

Griese M. Pulmonary surfactant in health and human lung diseases: state of the art. Eur Respir J. 1999;13:1455–76. https://doi.org/10.1183/09031936.99.13614779

Guillot L, Nathan N, Tabary O, Thouvenin G, Le Rouzic P, Corvol H, et al. Alveolar epithelial cells: master regulators of lung homeostasis. Int J Biochem Cell Biol. 2013;45:2568–73. https://doi.org/10.1016/j.biocel.2013.08.009

Gustafsson M, Griffiths WJ, Furusjö E, Johansson J. The palmitoyl groups of lung surfactant protein C reduce unfolding into a fibrillogenic intermediate. J Mol Biol. 2001;310:937–50. https://doi.org/10.1006/jmbi.2001.4810

Haugland RP. Handbook of fluorescent probes and research products. Molecular Probes; Pennsylvania State University, 2002.

Hiatt SM, Shyu YJ, Duren HM, Hu CD. Bimolecular fluorescence complementation (BiFC) analysis of protein interactions in *Caenorhabditis elegans*. Methods. 2008;45:185–91. https://doi.org/10.1016/j.ymeth.2008.06.003

Horowitz AD, Baatz JE, Whitsett JA. Lipid effects on aggregation of pulmonary surfactant protein SP-C studied by fluorescence

energy transfer. Biochemistry. 1993;32:9513–23. https://doi.org/10.1021/bi00088a001

Jia Y, Bleicher F, Reboulet J, Merabet S. Bimolecular fluorescence complementation (BiFC) and multiplexed imaging of protein-protein interactions in human living cells. Methods Mol Biol. 2021;2350:173–90. https://doi.org/10.1007/978-1-0716-1593-5_12

Johansson H, Eriksson M, Nordling K, Presto J, Johansson J. The Brichos domain of prosurfactant protein C can hold and fold a transmembrane segment. Protein Sci. 2009;18:1175–82. https://doi.org/10.1002/pro.123

Johansson J. Structure and properties of surfactant protein C. Biochim Biophys Acta. 1998;1408:161–72. https://doi.org/10.1016/s0925-4439(98)00065-9

Johansson J. Membrane properties and amyloid fibril formation of lung surfactant protein C. Biochem Soc Trans. 2001;29:601–6. https://doi.org/10.1042/bst0290601

Johansson J, Szyperski T, Curstedt T, Wüthrich K. The NMR structure of the pulmonary surfactant-associated polypeptide SP-C in an apolar solvent contains a valyl-rich alpha-helix. Biochemistry. 1994;33:6015–23. https://doi.org/10.1021/bi00185a042

Johansson J, Weaver TE, Tjernberg LO. Proteolytic generation and aggregation of peptides from transmembrane regions: lung surfactant protein C and amyloid beta-peptide. Cell Mol Life Sci. 2004;61:326–35. https://doi.org/10.1007/s00018-003-3274-6

Kairys V, Gilson MK, Luy B. Structural model for an AxxxG-mediated dimer of surfactant-associated protein C. Eur J Biochem. 2004;271:2086–92. https://doi.org/10.1111/j.1432-1033.2004.04107.x

Kang Y-F, Chen W-K, Teng K-X, Wang L-Y, Xu X-C, Niu L-Y, et al. Aggregation turns BODIPY fluorophores into photosensitizers: reversibly switching intersystem crossing on and off for smart photodynamic therapy. CCS Chem. 2022;4:3516–28. https://doi.org/10.31635/ccschem.021.202101600

Keating E, Zuo YY, Tadayyon SM, Petersen NO, Possmayer F, Veldhuizen RA. A modified squeeze-out mechanism for generating high surface pressures with pulmonary surfactant. Biochim Biophys Acta. 2012;1818:1225–34. https://doi.org/10.1016/j.bbamem.2011.12.007

Korolainen H, Lolicato F, Enkavi G, Pérez-Gil J, Kulig W, Vattulainen I. Dimerization of the pulmonary surfactant protein C in a membrane environment. PLoS One. 2022;17:e0267155. https://doi.org/10.1371/journal.pone.0267155

Liu Z, Jiang Z, Yan M, Wang X. Recent progress of BODIPY dyes with aggregation-induced emission. Front Chem. 2019;7:712. https://doi.org/10.3389/fchem.2019.00712

Loura LM, Fedorov A, Prieto M. Resonance energy transfer in a model system of membranes: application to gel and liquid crystalline phases. Biophys J. 1996;71:1823–36. https://doi.org/10.1016/S0006-3495(96)79383-9

Loura LMS, Fedorov A, Prieto M. Membrane probe distribution heterogeneity: a resonance energy transfer study. J Phys Chem B. 2000;104:6920–31. https://doi.org/10.1021/jp000246q

Loura LMS, Prieto M. Resonance energy transfer in heterogeneous planar and bilayer systems: theory and simulation. J Phys Chem B. 2000;104:6911–9. https://doi.org/10.1021/jp000245y

Lukovic D, Plasencia I, Taberner FJ, Salgado J, Calvete JJ, Pérez-Gil J, et al. Production and characterisation of recombinant forms of human pulmonary surfactant protein C (SP-C): structure and surface activity. Biochim Biophys Acta. 2006;1758:509–18. https://doi.org/10.1016/j.bbamem.2006.03.005

Luy B, Diener A, Hummel RP, Sturm E, Ulrich WR, Griesinger C. Structure and potential C-terminal dimerization of a recombinant mutant of surfactant-associated protein C in chloroform/-methanol. Eur J Biochem. 2004;271:2076–85. https://doi.org/10.1111/j.1432-1033.2004.04106.x

Marquardt DW. An algorithm for least-squares estimation of non-linear parameters. J Soc Ind Appl Math. 1963;11:431–41. https://doi.org/10.1137/0111030

Mason RJ, Greene K, Voelker DR. Surfactant protein A and surfactant protein D in health and disease. Am J Physiol. 1998;275:L1–L13. https://doi.org/10.1152/ajplung.1998.275.1.L1

Nogee LM, Garnier G, Dietz HC, Singer L, Murphy AM, DeMello DE, et al. A mutation in the surfactant protein B gene responsible for fatal neonatal respiratory disease in multiple kindreds. J Clin Invest. 1994;93:1860–3. https://doi.org/10.1172/JCI117173

Olmeda B, Martinez-Calle M, Perez-Gil J. Pulmonary surfactant metabolism in the alveolar airspace: biogenesis, extracellular conversions, recycling. Ann Anat. 2017;209:78–92. https://doi.org/10.1016/j.aanat.2016.09.008

Pakhomov AA, Deyev IE, Ratnikova NM, Chumakov SP, Mironiuk VB, Kononevich YN, et al. BODIPY-based dye for no-wash live-cell staining and imaging. Biotechniques. 2017;63:77–80. https://doi.org/10.2144/000114577

Parra E, Pérez-Gil J. Composition, structure and mechanical properties define performance of pulmonary surfactant membranes and films. Chem Phys Lipids. 2015;185:153–75. https://doi.org/10.1016/j.chemphyslip.2014.09.002

Pastrana-Rios B, Flach CR, Brauner JW, Mautone AJ, Mendelsohn R. A direct test of the "squeeze-out" hypothesis of lung surfactant function. External reflection FT-IR at the air/-water interface. Biochemistry. 1994;33:5121–7. https://doi.org/10.1021/bi00183a016

Perez-Gil J, Weaver TE. Pulmonary surfactant pathophysiology: current models and open questions. Physiology (Bethesda). 2010;25:132–41. https://doi.org/10.1152/physiol.00006.2010

Plasencia I, Cruz A, Casals C, Pérez-Gil J. Superficial disposition of the N-terminal region of the surfactant protein SP-C and the absence of specific SP-B-SP-C interactions in phospholipid bilayers. Biochem J. 2001;359:651–9. https://doi.org/10.1042/0264-6021:3590651

Plasencia I, Rivas L, Keough KM, Marsh D, Pérez-Gil J. The N-terminal segment of pulmonary surfactant lipopeptide SP-C has intrinsic propensity to interact with and perturb phospholipid bilayers. Biochem J. 2004;377:183–93. https://doi.org/10.1042/bj20030815

Roldan N, Goormaghtigh E, Perez-Gil J, Garcia-Alvarez B. Palmitoylation as a key factor to modulate SP-C-lipid interactions in lung surfactant membrane multilayers. Biochim Biophys Acta. 2015;1848:184–91. https://doi.org/10.1016/j.bbamem.2014.10.009

Roldan N, Nyholm TKM, Slotte JP, Perez-Gil J, Garcia-Alvarez B. Effect of lung surfactant protein SP-C and SP-C-promoted membrane fragmentation on cholesterol dynamics. Biophys J. 2016;111:1703–13. https://doi.org/10.1016/j.bpj.2016.09.016

Rouser G, Fkeischer S, Yamamoto A. Two dimensional then layer chromatographic separation of polar lipids and determination

of phospholipids by phosphorus analysis of spots. Lipids. 1970; 5:494–6. https://doi.org/10.1007/bf02531316

Sánchez-Pulido L, Devos D, Valencia A. BRICHOS: a conserved domain in proteins associated with dementia, respiratory distress and cancer. Trends Biochem Sci. 2002;27:329–32. https://doi.org/10.1016/s0968-0004(02)02134-5

Sarabipour S, Hristova K. Glycophorin a transmembrane domain dimerization in plasma membrane vesicles derived from CHO, HEK 293T, and A431 cells. Biochim Biophys Acta. 1828;2013: 1829–33. https://doi.org/10.1016/j.bbamem.2013.03.022

Sehlmeyer K, Ruwisch J, Roldan N, Lopez-Rodriguez E. Alveolar dynamics and beyond – the importance of surfactant protein C and cholesterol in lung homeostasis and fibrosis. Front Physiol. 2020;11:386. https://doi.org/10.3389/fphys.2020.00386

Serrano AG, Pérez-Gil J. Protein-lipid interactions and surface activity in the pulmonary surfactant system. Chem Phys Lipids. 2006;141:105–18. https://doi.org/10.1016/j.chemphyslip.2006.02.017

Silveyra P, Floros J. Genetic variant associations of human SP-A and SP-D with acute and chronic lung injury. Front Biosci. 2012;17:407–29. https://doi.org/10.2741/3935

Szyperski T, Vandenbussche G, Curstedt T, Ruysschaert JM, Wüthrich K, Johansson J. Pulmonary surfactant-associated polypeptide C in a mixed organic solvent transforms from a monomeric alpha-helical state into insoluble beta-sheet aggregates. Protein Sci. 1998;7:2533–40. https://doi.org/10.1002/pro.5560071206

Taeusch HW, Bernardino de la Serna J, Perez-Gil J, Alonso C, Zasadzinski JA. Inactivation of pulmonary surfactant due to serum-inhibited adsorption and reversal by hydrophilic polymers: experimental. Biophys J. 2005;89:1769–79. https://doi.org/10.1529/biophysj.105.062620

ten Brinke A, Vaandrager AB, Haagsman HP, Ridder AN, van Golde LM, Batenburg JJ. Structural requirements for palmitoylation of surfactant protein C precursor. Biochem J. 2002;361: 663–71. https://doi.org/10.1042/0264-6021:3610663

ten Brinke A, van Golde LM, Batenburg JJ. Palmitoylation and processing of the lipopeptide surfactant protein C. Biochim Biophys Acta. 2002;1583:253–65. https://doi.org/10.1016/s1388-1981(02)00248-2

Tokieda K, Whitsett JA, Clark JC, Weaver TE, Ikeda K, McConnell KB, et al. Pulmonary dysfunction in neonatal SP-B-deficient mice. Am J Physiol. 1997;273:L875–82. https://doi.org/10.1152/ajplung.1997.273.4.L875

Traïkia M, Warschawski DE, Recouvreur M, Cartaud J, Devaux PF. Formation of unilamellar vesicles by repetitive freeze-thaw cycles: characterization by electron microscopy and 31P-nuclear magnetic resonance. Eur Biophys J. 2000;29:184–95. https://doi.org/10.1007/s002490000077

Umberger JQ, Lamer VK. The kinetics of diffusion controlled molecular and ionic reactions in solution as determined by measurements of the quenching of fluorescence. J Am Chem Soc. 1945;67:1099–109. https://doi.org/10.1021/ja01223a023

Vandenbussche G, Clercx A, Curstedt T, Johansson J, Jornvall H, Ruysschaert JM. Structure and orientation of the surfactant-associated protein C in a lipid bilayer. Eur J Biochem. 1992;203: 201–9. https://doi.org/10.1111/j.1432-1033.1992.tb19848.x

Wang WJ, Russo SJ, Mulugeta S, Beers MF. Biosynthesis of surfactant protein C (SP-C). Sorting of SP-C proprotein involves homomeric association via a signal anchor domain. J Biol Chem. 2002;277:19929–37. https://doi.org/10.1074/jbc.M201537200

Wang Z, Gurel O, Baatz JE, Notter RH. Acylation of pulmonary surfactant protein-C is required for its optimal surface active interactions with phospholipids. J Biol Chem. 1996;271:19104–9. https://doi.org/10.1074/jbc.271.32.19104

Weaver TE. Synthesis, processing and secretion of surfactant proteins B and C. Biochim Biophys Acta. 1998;1408:173–9. https://doi.org/10.1016/s0925-4439(98)00066-0

Wüstneck N, Wüstneck R, Perez-Gil J, Pison U. Effects of oligomerization and secondary structure on the surface behavior of pulmonary surfactant proteins SP-B and SP-C. Biophys J. 2003;84: 1940–9. https://doi.org/10.1016/s0006-3495(03)75002-4

SUPPORTING INFORMATION

Additional supporting information can be found online in the Supporting Information section at the end of this article.

How to cite this article: Morán-Lalangui M, Coutinho A, Prieto M, Fedorov A, Pérez-Gil J, Loura LMS, et al. Exploring protein–protein interactions and oligomerization state of pulmonary surfactant protein C (SP-C) through FRET and fluorescence self-quenching. Protein Science. 2024;33(1):e4835. https://doi.org/10.1002/pro.4835